Available online at www.sciencedirect.com
ScienceDirect
Polymer 48 (2007) 1075–1082
polymer
www.elsevier.com/locate/polymer

Effect of nanoplatelet aspect ratio on mechanical properties of epoxy nanocomposites

W.-J. Boo [a], L. Sun [a,b], G.L. Warren [a], E. Moghbelli [a], H. Pham [c], A. Clearfield [b], H.-J. Sue [a,*]

[a] Polymer Technology Center, Department of Mechanical Engineering, Texas A&M University, College Station, TX 77843-3123, United States
[b] Department of Chemistry, Texas A&M University, College Station, TX 77842-3012, United States
[c] Resins R&D, The Dow Chemical Company, Freeport, TX 77541, United States

Received 23 October 2006; received in revised form 19 December 2006; accepted 21 December 2006
Available online 4 January 2007

Abstract

To study the effect of the aspect ratio of nanoplatelets on the mechanical properties of polymer nanocomposites, epoxy/α-zirconium phosphate nanocomposites with two distinctive aspect ratios at ca. 100 and 1000 have been prepared and characterized. Scanning electron microscopy and transmission electron microscopy were utilized to confirm the two different sizes and aspect ratios of nanoplatelets in epoxy. As expected, it is found that mechanical properties of the nanocomposite are affected by the aspect ratio of nanoplatelets in epoxy. That is, a higher aspect ratio renders a better improvement in modulus. It is also found that the interfacial characteristics between the nanoplatelets and polymer matrix are most critical in affecting the strength and ductility of the polymer. The operative fracture mechanisms depend strongly on the aspect ratio of the nanoplatelets incorporated. The crack deflection mechanism, which leads to a tortuous path crack growth, is only observed for the high aspect ratio system. The implication of the present findings for structural applications of polymer nanocomposites is discussed.

Keywords: Polymer nanocomposite; α-Zirconium phosphate; Aspect ratio

1. Introduction

Since the successful development of nylon/clay nanocomposites that showed great improvements in physical and mechanical properties with only a small amount of clay introduced into the polymer matrix [1–3] in the late 1980s, the pursuits for high performance polymer nanocomposites have swamped both the scientific community and the industry in the past two decades. Numerous research efforts in this field have been focused on the incorporation of nanoplatelet fillers to greatly enhance their physical, mechanical, and chemical properties in various polymer matrices, including epoxy [4,5], polypropylene [6–8], polyethylene [9], polyimide [10,11], polystyrene [12–14], poly(methyl methacrylate) [15], etc. Most results have revealed great improvements of polymer properties by a small addition of nanoplatelets (<5 wt%). Important factors that can affect the physical and mechanical properties of nanoplatelet-reinforced polymer nanocomposites include nanoplatelets type [16–20], intercalating agents [21–24], filler loading levels [25–27], and processing [28,29]. In particular, significant efforts have emphasized on achieving maximum level of exfoliation of nanoplatelets in polymer matrices.

Recently, more emphases have been placed on investigating how the nanoplatelet aspect ratio, defined as the ratio of the long axis to platelet thickness, affects the physical and mechanical properties of polymer nanocomposites. For example, Maiti et al. [30] synthesized polylactide/layered silicate nanocomposites using organic phosphonium intercalating agents with different chain lengths to reveal the influence of nanoplatelet size and aspect ratio on the properties of polymer nanocomposites. To obtain exfoliated nanoplatelets with

* Corresponding author. Tel.: +1 979 845 5024; fax: +1 979 862 3989.
E-mail address: hjsue@tamu.edu (H.-J. Sue).

0032-3861/$ - see front matter © 2007 Elsevier Ltd. All rights reserved.
doi:10.1016/j.polymer.2006.12.042

variations in aspect ratio in polymer matrices, they employed smectite, montmorillonite, and mica as nanofillers. Depending on the size of each type of layered silicates incorporated, the effects of dispersion, intercalation, and aspect ratio of nanoplatelets on mechanical and gas barrier properties of nanocomposites were investigated. More recently, Osman et al. [31] used *n*-benzyldimethyl hexadecylammonium to intercalate and exfoliate montmorillonite clay in epoxy and polyurethane matrices, respectively, to investigate their gas barrier properties. The aspect ratios of the organoclay were varied by controlling the level of intercalation and exfoliation of the clay in the polymer matrix.

It should be pointed out that the above studies were performed based on the use of different types of natural silicates [30,32] or the use of different intercalating agents to obtain different filler aspect ratios in the nanocomposites. Consequently, in addition to the aspect ratio effect, uncertainties on the effect of different types of silicates and intercalating agents were introduced. Thus, it is unlikely that unambiguous results on how the aspect ratio of nanoplatelets affect physical and mechanical properties can be obtained.

Recently, alternative approaches have been undertaken to definitively investigate how the nanoplatelet size and aspect ratio influence the physical and mechanical properties of polymer nanocomposites. To avoid any possible ambiguities accompanied by the utilization of different fillers and surface functionalities to achieve the control of aspect ratios, synthetic α-zirconium phosphate (α-ZrP), $Zr(HPO_4)_2 \cdot H_2O$, that possesses well-controlled sizes and aspect ratios was prepared. The advantages of α-ZrP over that of clay have been highlighted elsewhere [33–38]. They will not be elaborated here. Because of the unique attributes of α-ZrP, a series of fundamental studies, including (1) the synthesis, intercalation, and exfoliation of α-ZrP [36,38,39] in epoxy, (2) the preparation of exfoliated epoxy/α-ZrP nanocomposites [40], and (3) the study of fracture behaviors of epoxy/α-ZrP [41–43] with various degrees of exfoliation have been carried out recently. Insightful information has been obtained.

In this work, fundamental study on how the nanoplatelet aspect ratio influences the mechanical properties of polymer nanocomposites was conducted. Considering the structure of nanoplatelet particles, it is expected that the higher aspect ratio of nanoplatelets will be more effective for the enhancement of mechanical properties due to the higher surface area of the nanoplatelets.

Instead of using high molecular weight monoamines, a small amount of less reactive intercalating agent, tetra-*n*-butyl ammonium hydroxide (TBA), is utilized [44] to minimize unintended reaction of intercalating agent with epoxy monomer. As a result, the glass transition temperature (T_g) of nanoplatelet-reinforced polymer nanocomposites can be maintained. Furthermore, the effect of intercalating agent type on mechanical properties of nanocomposite can be addressed by comparing the present findings against our earlier results where long-chain monoamine was utilized [41]. The usefulness of high aspect ratio nanoplatelets in polymer nanocomposites for structural applications is also discussed.

2. Experimental

2.1. Materials

The materials used in this study are listed in Table 1. Two α-ZrP having two different aspect ratios, i.e., ca. 100 and 1000, were synthesized [39]. The detailed chemistry and procedures for the synthesis and control of aspect ratio of α-ZrP can be found elsewhere [33–36,38,39]. TBA (tetra-*n*-butyl ammonium hydroxide $[(CH_3CH_2CH_2CH_2)_4N(OH)$, Aldrich] was used as surface modifiers to intercalate α-ZrP layers. The diglycidyl ether of bisphenol-A (DGEBA) epoxy resin (D.E.R.™ 332 epoxy resin, The Dow Chemical Company), which has a narrow monomer molecular weight distribution (172–176 g/mol), was used in this study. The curing agent utilized is 4,4′-diaminodiphenylsulfone (DDS, Aldrich). All the chemicals were used as received except epoxy resin, which was dried in a vacuum oven for 24 h prior to sample preparation.

2.2. Preparation of epoxy/α-ZrP nanocomposites

The interlayer *d*-spacing of pristine α-ZrP is known to be 7.6 Å [40]. The addition of TBA at a 0.75:1 molar ratio in deionized water at 0 °C can lead to full exfoliation of α-ZrP layers into individual nanoplatelets. Detailed sample preparation procedures for achieving fully exfoliated α-ZrP in water and in epoxy can be found elsewhere [36].

After exfoliation in deionized water, α-ZrP nanoplatelets with aspect ratios of ca. 100 and 1000 were washed and transferred into acetone with an aid of centrifuge [36]. DGEBA epoxy monomer which was pre-dissolved in acetone was added to achieve a final inorganic α-ZrP loading of 0.7 vol% in epoxy. After removal of solvent with Rotarvapor® in a water bath at about 90 °C, DDS was added at stoichiometric ratio. After the DDS melted at 130 °C, the resin mixture was cast in a preheated glass mold and cured in an oven at 180 °C for 2 h, followed by 2 h of post-cure at 220 °C. The epoxy/α-ZrP systems with aspect ratios of 100 and 1000 are designated as epoxy/ZrP-100 and epoxy/ZrP-1000, respectively. For comparison, a neat epoxy plaque (neat epoxy) and an epoxy plaque with only intercalating agent, i.e., TBA, addition (epoxy/TBA) were also prepared.

Table 1
Material specification and source

Material	Comments/specifications	Supplier
α-ZrP-100	Phosphoric acid (3 M), refluxing at 100 °C, aspect ratio 100	Synthesized in PTC[a]
α-ZrP-1000	Hydrofluoric acid, hydrothermal condition, aspect ratio 1000	Synthesized in PTC
Intercalating agent	Tetra-*n*-butyl ammonium hydroxide (TBA)	Aldrich
Epoxy resin	D.E.R.™ 332, diglycidyl ether of bisphenol-A (DGEBA)	DOW Chemical
Curing agent	DDS, 4,4′-diamino-diphenyl sulfone	Aldrich

[a] Polymer Technology Center, Texas A&M University.

It should be noted that attempts were made to increase the α-ZrP loading in epoxy. However, when α-ZrP loading is greater than 0.7 vol% for the epoxy/α-ZrP-1000 system, the viscosity build-up will become so high that good quality epoxy nanocomposite plaques cannot be prepared. As a result, only epoxy nanocomposite panels with 0.7 vol% of α-ZrP were investigated.

2.3. Morphology characterization

Scanning electron microscopic (SEM) images of α-ZrP nanoplatelets were acquired using a Zeiss Leo 1530 VP Field Emission-SEM (FE-SEM). The samples were sputter-coated with a thin layer (ca. 3 nm) of Pt/Pd (80/20) prior to SEM observation. For transmission electron microscopic (TEM) observation, the thin-section samples extracted from the core region of the specimens were prepared by microtoming (Ultracut E) and the thin sections (~100 nm thickness) were deposited on carbon coated Cu grids. Sample grids were examined on a JEOL 1200 EX electron microscope operated at an accelerating voltage of 100 kV. TEM micrographs were printed on a calibrated Kodak® electron microscope film. Complete details of the microtomy and microscopy techniques employed here are given in prior publications [40–43].

2.4. Mechanical properties and fracture behavior studies

Tensile properties of epoxy nanocomposites reinforced with α-ZrP having two different aspect ratios were obtained based on the ASTM D638-98 method. The tensile tests were performed using an MTS® servo-hydraulic test machine at a crosshead speed of 5.08 mm/min at ambient temperature. Young's modulus, tensile strength, and elongation-at-break of each sample were obtained based on at least five specimens per sample and the average values and standard deviations were reported.

Dynamic mechanical analysis (DMA) was conducted on a RSA III (TA Instruments) with a 3-point-bending mode, at a fixed frequency of 1 Hz and with a temperature increase of 5 °C per step, ranging from −150 to 250 °C. A sinusoidal strain–amplitude of 0.05% was chosen for the measurement. The maximum point on the tan δ curve was recorded as the T_g of the samples. Multiple scans were conducted to ensure reproducibility.

Fracture toughness tests were conducted based on the linear elastic fracture mechanics (LEFM) approach. The single-edge-notch 3-point-bending (SEN-3PB) test, based on ASTM D5045-96, was performed to obtain the mode-I critical stress intensity factor (K_{IC}) of the neat epoxy and epoxy nanocomposites with two different aspect ratios. Care was taken to ensure that the initial sharp crack, generated by tapping with a fresh razor blade, exhibited a thumbnail shape crack front prior to testing. At least five specimens per sample were tested to determine K_{IC} values of the samples. The critical stress intensity factors were calculated using the following equation:

$$K_{IC} = \frac{P_C S}{BW^{3/2}} f(a/W) \quad (1)$$

where P_C is the load at crack initiation, S is the span width, B is the thickness of the specimen, W is the width of the specimen, and a is the initial crack length.

The double-notch 4-point-bending (DN-4PB) test was conducted to probe the detailed mechanisms on crack propagation phenomena in the epoxy nanocomposites with variation in filler aspect ratios. Detailed methods of sample preparation and testing can be found elsewhere [45,46]. The DN-4PB tests were performed at ambient temperature. The arrested subcritical crack tip damage zone from the core region of the specimen was isolated, trimmed, and thin-sectioned for TEM observation.

3. Results and discussion

3.1. Morphology characterization

After synthesis, washing, and drying the powder of crystalline α-ZrP, SEM was employed to verify the size of the nanoplatelets synthesized. Fig. 1 displays the SEM micrographs of the α-ZrP nanoplatelets with their aspect ratios of (a) 100 and (b) 1000.

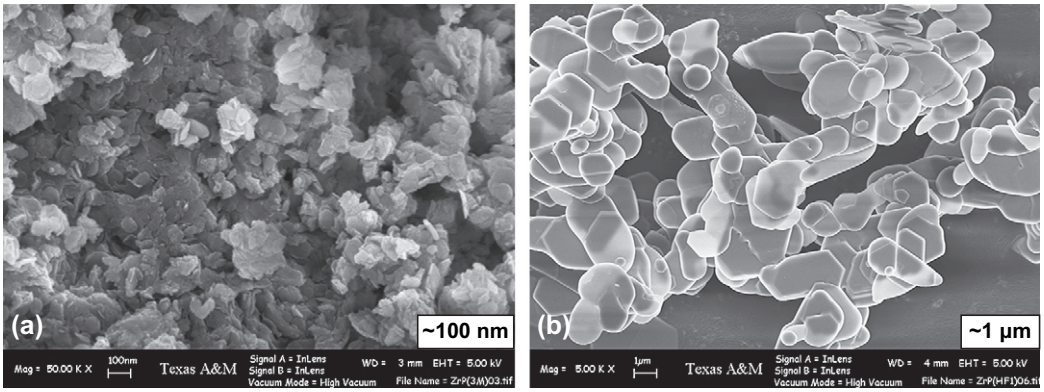

Fig. 1. SEM of α-ZrP nanoplatelets having aspect ratios of: (a) 100 and (b) 1000.

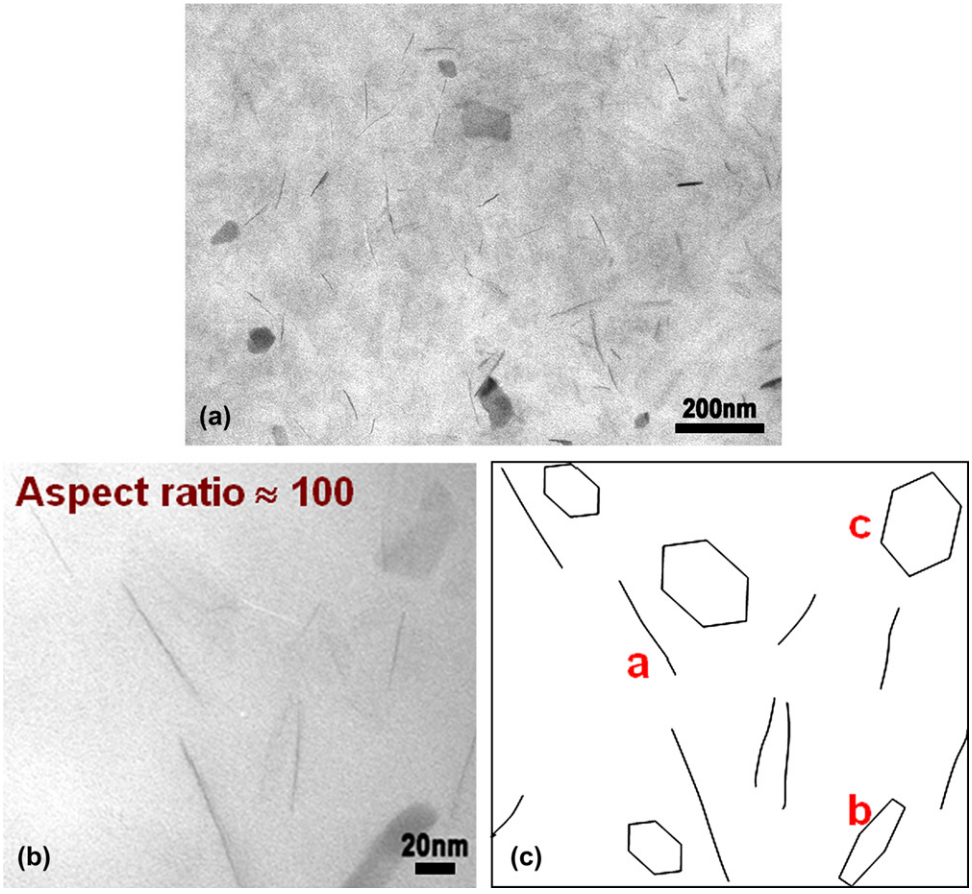

Fig. 2. TEM of epoxy/ZrP-100 nanocomposite: (a) low magnification, (b) high magnification, and (c) the corresponding schematic.

Since all the detailed XRD patterns of intercalated and exfoliated α-ZrP with various aspect ratios and those of corresponding nanocomposites can be found elsewhere [36,39,41,42], only TEM micrographs of epoxy/α-ZrP nanocomposites are reported here. According to the XRD characterization in the previous reports [36,39,41,42], fully exfoliated α-ZrP layer in epoxy is obtained. To directly confirm the state of exfoliation and an overall dispersion of exfoliated α-ZrP nanoplatelets in epoxy matrix, the samples were imaged by TEM.

Fig. 2(a) displays highly exfoliated and well-dispersed α-ZrP-100 nanoplatelets (0.7 vol%) in epoxy. The TEM image clearly shows random orientation of α-ZrP nanoplatelets which are completely exfoliated. This random orientation is probably due to the low filler loading (0.7 vol%). In contrast, locally oriented nanoplatelet morphology has been observed at higher α-ZrP loadings [40,42]. Furthermore, the frequency of α-ZrP oriented parallel to the thin-section direction, i.e., the surface of the micrograph, appears to be higher than that of the 1 and 2 vol% loading scenarios [41,42]. Fig. 2(b) presents a high magnification TEM image of epoxy/α-ZrP from the same sample. As shown, the nanoplatelets show different morphology due to random orientation. The schematic in Fig. 2(c) aids to demonstrate the various orientations of nanoplatelets in detail: noted as *a*, *b*, and *c*. The α-ZrP nanoplatelets can appear as straight lines, tilted surfaces, or fully exposed flat surfaces.

In Fig. 3(a), high aspect ratio α-ZrP-1000 nanoplatelets also show complete exfoliation and random orientation in epoxy matrix. However, it is interesting to note that the high aspect ratio α-ZrP nanoplatelets exhibit a strong curvature instead of being straight. The high magnification TEM image in Fig. 3(b) shows a curved platelet. As depicted in *d*, *e*, and *f* (Fig. 3(c)), a single large nanoplatelet can appear as a straight line, a curved line in-between, and a tilted surface at different locations of the TEM thin section. No evidence of completely flat ZrP-1000 is found in the thin section, probably because the TEM thin section is too thin ($\approx$80 nm) to accommodate a complete curved α-ZrP nanoplatelet ($\approx$1000 nm) in the same thin section.

As pointed out earlier, the incorporation of 0.7 vol% of high aspect ratio α-ZrP in epoxy can drastically increase the viscosity of epoxy, making it extremely difficult to prepare void free epoxy plaques. As a result, only 0.7 vol% was incorporated in epoxy for this study.

3.2. Mechanical property characterization

The tensile properties of epoxy/ZrP-100 and epoxy/ZrP-1000 are summarized in Table 2. For comparison purposes, the plaques of neat epoxy (DGEBA/DDS) and an intercalating agent containing neat epoxy (epoxy/TBA) were also tested and compared. The tensile modulus of epoxy/ZrP-100 is found to

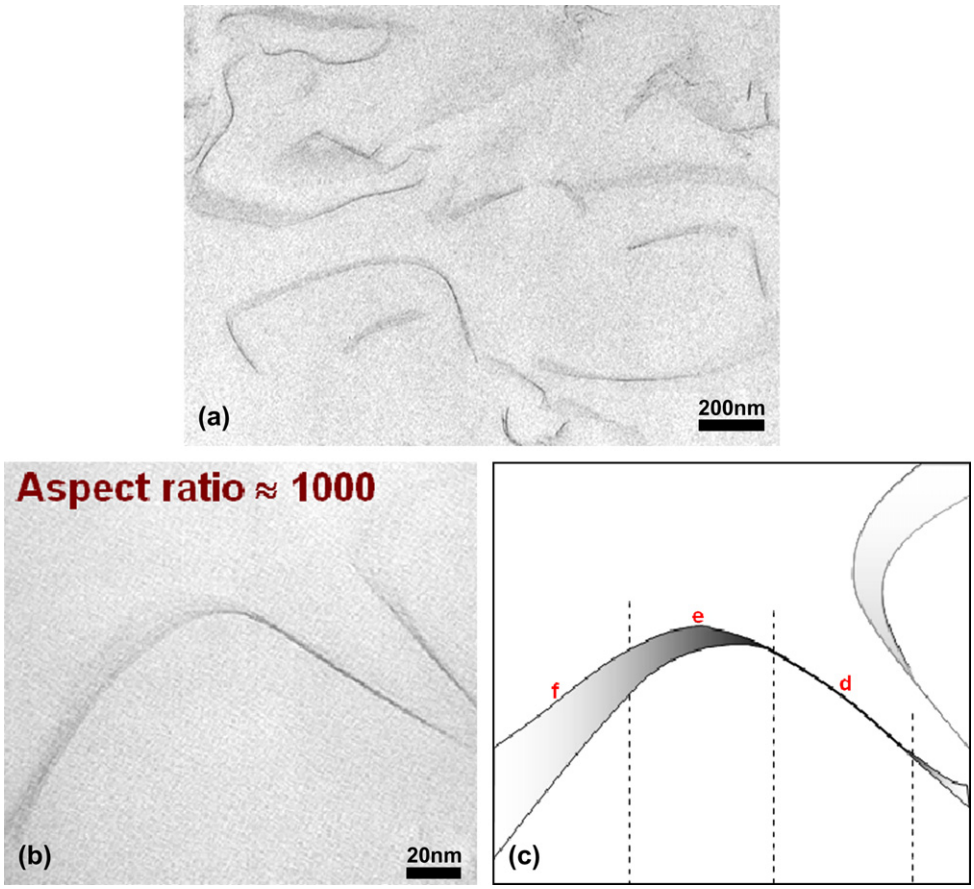

Fig. 3. TEM of epoxy/ZrP-1000 nanocomposite: (a) low magnification, (b) high magnification, and (c) the corresponding schematic.

increase only by 5% due to the low level of loading. Whereas, in the case of epoxy/ZrP-1000, an increase of about 12% in modulus is observed under the same condition. The larger increase in tensile modulus is explained from the higher aspect ratio of α-ZrP nanoplatelets. The decrease in elongation-at-break is greater for the high aspect ratio case and the trends correspond well with the results of Ray et al. [32].

It should be noted that the tensile strength and elongation-at-break of both low and high aspect ratio cases are decreased due to the incorporation of the well-dispersed ZrP nanoplatelets. This finding is different from our earlier finding [41], which indicates that both strength and ductility of the epoxy nanocomposite can be maintained when the intercalating agent utilized is long-chain monoamine-based. This clearly suggests that the type of intercalating agent utilized can have a significant impact on the strength and ductility of the polymer nanocomposites. This point will be further discussed later.

Fig. 4 shows DMA spectra of neat epoxy, epoxy/ZrP-100, and epoxy/ZrP-1000. The overall DMA behavior is consistent with our previous findings [38,42]. For comparison purposes, epoxy that contains intercalating agent (epoxy/TBA) was also tested and exhibits a T_g of 195 °C (not shown). It is evident that the use of TBA as an intercalating agent is better for maintaining the T_g of epoxy than the long-chain monoamines [40–43]. It should be noted that the T_g of the epoxy/ZrP-100 and epoxy/ZrP-1000 is found to be 200 and 204 °C, respectively. The above finding implies that the aspect ratio of the nanoplatelet does not play a significant role in affecting T_g at low nanoplatelet loadings. It appears that the incorporation of intercalating agent (surface modifier) may have a more significant effect on T_g for epoxy, simply because of the participation of the intercalating agent in the curing of epoxy.

By comparing the tensile and DMA results of the current epoxy nanocomposites that use TBA as intercalating agent

Table 2
Tensile properties and fracture toughness of epoxy/α-ZrP nanocomposites

	Neat epoxy	Epoxy/ZrP-100	Epoxy/ZrP-1000	Epoxy/TBA
Young's modulus (GPa)	2.90 ± 0.05	3.04 ± 0.12	3.25 ± 0.19	2.89 ± 0.13
Tensile strength (MPa)	75.3 ± 6.4	54.7 ± 4.9	46.0 ± 4.4	43.2 ± 4.3
Elongation-at-break (%)	4.1 ± 0.4	2.5 ± 0.4	1.9 ± 0.2	2.3 ± 0.5
K_{IC} (MPa m$^{1/2}$)	0.72 ± 0.02	0.58 ± 0.01	0.69 ± 0.02	0.61 ± 0.02

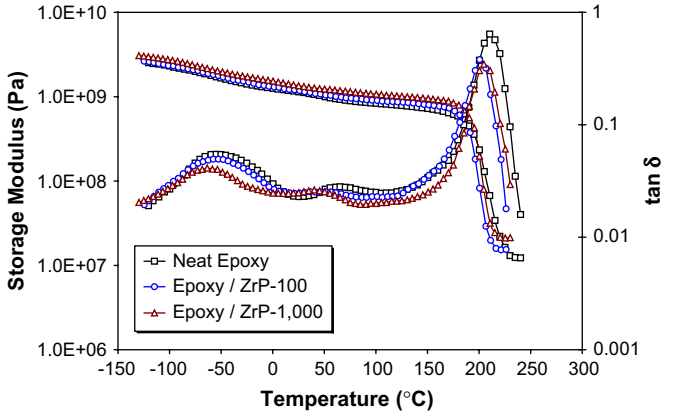

Fig. 4. DMA results of neat epoxy and epoxy nanocomposites.

and the previous nanocomposites that use monoamines as intercalating agent [40–43], it is evident that the T_g, strength, and ductility of the epoxy nanocomposite can be greatly influenced by the type of intercalating agents utilized. For instance, in our previous results [40–43], a significant T_g drop has been observed due to the unintended reaction between the monoamine intercalating agent and epoxy monomers. However, the nanocomposites in this study utilize TBA as an intercalating agent and show that the T_g of the epoxy nanocomposite remains close to that of the neat epoxy.

Upon the use of TBA, the tensile strength and ductility of the epoxy nanocomposite are decreased. These drop in strength and ductility can be attributed not only to a more complete curing of epoxy with DDS but also to the more rigid interface between the polymer and the nanoplatelets, which restricts the segmental motion near the organic–inorganic interfaces [47]. The above hypothesis finds supports from the work of Kim et al. [44] and Ha et al. [48]. When TBA and monoamine are bonded to α-ZrP, TBA creates less flexible interface than monoamine-terminated polyether chains on and around α-ZrP layers. Fig. 5 shows the molecular structures of the TBA utilized in this study and the monoamine-terminated polyether used in our previous reports [41,42]. As shown in Fig. 5(a), TBA has a much shorter aliphatic chain. They can be tightly packed and exhibit less flexibility, as opposed to the long single-chain monoamine structure (Fig. 5(b)).

3.3. Fracture behavior study

The mode-I fracture toughness (K_{IC}) values of epoxy/ZrP-100 and epoxy/ZrP-1000 are measured and are listed in Table 2. A neat epoxy and an epoxy/TBA are also tested as a control. As shown in Table 2, there is no substantial difference in K_{IC} values between neat epoxy and epoxy/ZrP-100. This result is consistent with our earlier study on both clay-filled and ZrP-reinforced epoxy nanocomposite systems [49]. In the case of epoxy/ZrP-1000, K_{IC} value is slightly higher than epoxy/ZrP-100. However, the difference is still limited. To investigate the fracture mechanisms in epoxy nanocomposites, the DN-4PB tests were carried out on epoxy/ZrP-100 and epoxy/ZrP-1000. TEM images from the arrested crack tip and crack wake are given in Figs. 6 and 7, respectively.

As shown in Fig. 6, when the nanoplatelets are fully exfoliated, the subcritically propagated crack would grow more or less in a straight fashion. No signs of delamination or crack deflection can be found. This explains why the fracture toughness (K_{IC}) value is about the same as neat epoxy. This finding is also in good agreement with our previous results with various loading levels of α-ZrP in epoxy [41,42].

In the case of epoxy/ZrP-1000, significant crack deflection, crack bifurcation, and microcracking are observed (Fig. 7). Fig. 7(a) and (b) is TEM taken from the crack wake, showing

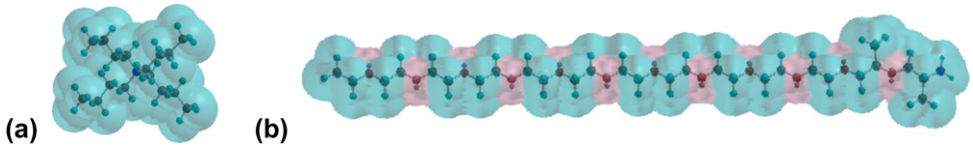

Fig. 5. Molecular structure and size comparison of the intercalating agents between (a) tetra-*n*-butyl ammonium hydroxide and (b) monoamine-terminated polyether.

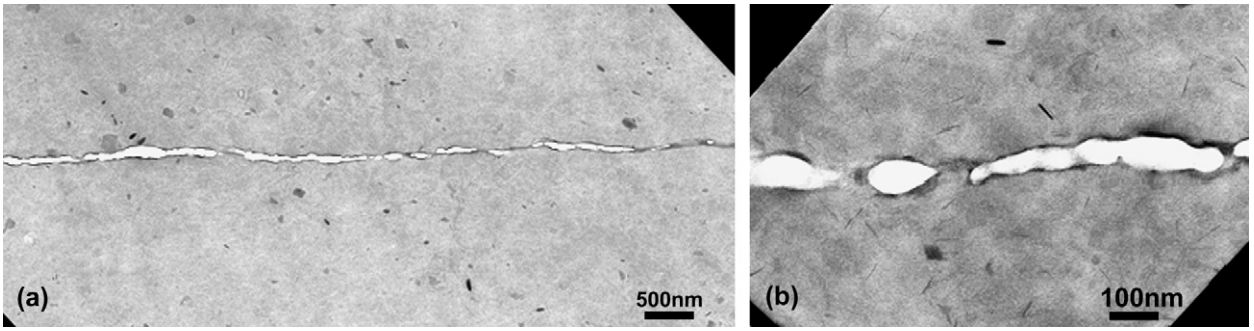

Fig. 6. TEM of DN-4PB damage zone of epoxy/ZrP-100: (a) the crack wake and (b) the crack tip region. The crack propagates from left to right.

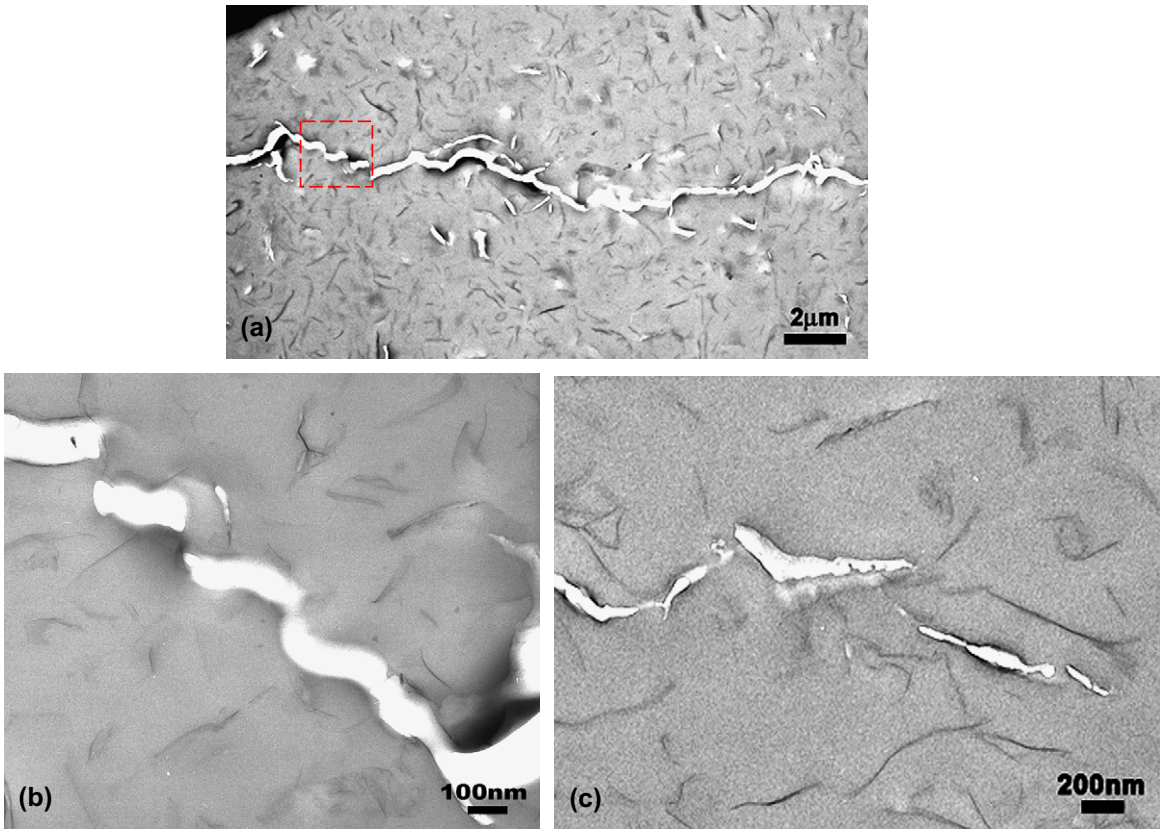

Fig. 7. TEM of DN-4PB damage zone of epoxy/ZrP-1000 nanocomposite: (a) the crack wake region (low magnification), (b) the crack wake region (high magnification), and (c) the crack tip region. The crack propagates from left to right.

significant crack deflection at low and high magnifications, respectively. As shown in Fig. 7(c), the crack appears to grow along the interface of α-ZrP layers, suggesting a poorer interfacial adhesive strength than the cohesive strength of the epoxy matrix. As mentioned earlier [41,42], if the α-ZrP nanoplatelet aspect ratio is around 100, the crack would propagate in a straight manner without sensing the presence of nanoplatelets. However, when the aspect ratio of the nanoplatelets becomes high, the crack begins to interact with the nanoplatelets to cause crack deflection, crack bifurcation, and even microcracking.

It should be noted that the crack deflection, crack bifurcation, and microcracking observed in epoxy/ZrP-1000 are not effective toughening mechanisms. These mechanisms are not as effective as shear banding or crazing [49]. Furthermore, in the case of the highly intercalated epoxy/α-ZrP nanocomposite, modified by monoamine intercalating agent, the crack deflection observed does not give rise to any noticeable increase in K_{IC} [41,43]. This may be due to the presence of monoamine intercalating agent which greatly weakens the delamination strength of the intercalated ZrP. As a result, the toughening effect due to crack deflection mechanism is cancelled out by the weakening of the intercalating layers ahead of the crack tip.

The present study clearly shows that, for polymer nanocomposite systems, the aspect ratio as well as the physical size of nanoplatelets can play an important role on their mechanical performance. Another important finding of the present study is that intercalating agent can greatly influence the mechanical properties of the polymer nanocomposites. Even though aspect ratio of the nanoplatelets does not show significant impact on the mechanical properties of epoxy due to their low loadings, it should be pointed out that aspect ratio is likely to significantly influence the gas barrier properties and rheological behavior of the polymer matrix. The effect of the types of intercalating agents and their loadings on the gas barrier properties and rheological behavior of polymer nanocomposites will be reported in the near future.

4. Conclusion

To understand how the aspect ratio of nanoplatelets affects the mechanical property of polymer nanocomposites, epoxy/α-ZrP nanocomposites with two different aspect ratios of 100 and 1000 were prepared and characterized. Morphological differences between two distinctive sets of epoxy/α-ZrP nanocomposites have been observed. Based on the present study, while the influence of aspect ratio on the mechanical properties is not significant due to the low loading level of nanoplatelets, it has a significant effect on the operative fracture mechanisms and dynamic mechanical behaviors. The present study also shows that intercalating agent can greatly influence the tensile strength and ductility of the polymer nanocomposites.

Acknowledgments

The authors would like to acknowledge *partial* financial supports of the Defense Logistic Agency (SP0103-02-D-0024), the State of Texas ARP Grant (000512-00311-2003), and National Science Foundation (DMR-0332453).

References

[1] Kojima Y, Usuki A, Kawasumi M, Okada A, Kurauchi T, Kamigaito O. J Polym Sci Part A Polym Chem 1993;31:983.
[2] Kojima Y, Usuki A, Kawasumi M, Okada A, Fukushima Y, Kurauchi T, et al. J Mater Res 1993;8:1185.
[3] Yano K, Usuki A, Okada A, Kurauchi T, Kamigaito O. J Polym Sci Polym Chem 1993;31:2493.
[4] Kinloch AJ, Taylor AC. J Mater Sci Lett 2003;22:1439.
[5] Liu TX, Tjiu WC, Tong YJ, He CB, Goh SS, Chung TS. J Appl Polym Sci 2004;94:1236.
[6] Hasegawa N, Okamoto H, Kato M, Usuki A. J Appl Polym Sci 2000;78: 1918.
[7] Kato M, Usuki A, Okada A. J Appl Polym Sci 1997;66:1781.
[8] Kawasumi M, Hasegawa N, Kato M, Usuki A, Okada A. Macromolecules 1997;30:6333.
[9] Chrissopoulou K, Altintzi I, Anastasiadis SH, Giannelis EP, Pitsikalis M, Hadjichristidis N, et al. Polymer 2005;46:12440.
[10] Lan T, Kaviratna PD, Pinnavaia TJ. Chem Mater 1994;6:573.
[11] Tyan HL, Liu YC, Wei KH. Chem Mater 1999;11:1942.
[12] Hasegawa N, Okamoto H, Kawasumi M, Usuki A. J Appl Polym Sci 1999;74:3359.
[13] Essawy HA, Badran AS, Youssef AM, Abd El Hakim AA. Macromol Chem Phys 2004;205:2366.
[14] Morgan AB, Harris JD. Polymer 2004;45:8695.
[15] Zhu J, Start P, Mauritz KA, Wilkie CA. Polym Degrad Stab 2002;77:253.
[16] Usuki A, Kojima Y, Kawasumi M, Okada A, Kurauchi T, Kamigaito O. Abstr Pap Am Chem Soc 1990;200:218.
[17] Skowronski JM, Shioyama H. Carbon 1995;33:1473.
[18] Shioyama H. Carbon 1997;35:1664.
[19] Harris DJ, Bonagamba TJ, Schmidt-Rohr K. Macromolecules 1999;32: 6718.
[20] Kellar JJ, Herpfer MA, Moudgil BM, Society for Mining Metallurgy and Exploration (U.S.). Functional fillers and nanoscale minerals. Littleton, Colo: Society for Mining Metallurgy and Exploration; 2003.
[21] Kim JK, Hu CG, Woo RSC, Sham ML. Compos Sci Technol 2005;65: 805.
[22] Wang Z, Pinnavaia TJ. Chem Mater 1998;10:1820.
[23] Hasegawa N, Kawasumi M, Kato M, Usuki A, Okada A. J Appl Polym Sci 1998;67:87.
[24] Liu J, Boo W-J, Clearfield A, Sue H-J. Mater Manuf Process 2005;20: 143.
[25] Lan T, Pinnavaia TJ. Chem Mater 1994;6:2216.
[26] Messersmith PB, Giannelis EP. Chem Mater 1994;6:1719.
[27] Giannelis EP. Adv Mater 1996;8:29.
[28] Okamoto M, Morita S, Taguchi H, Kim YH, Kotaka T, Tateyama H. Polymer 2000;41:3887.
[29] Weon JI, Sue HJ. Polymer 2005;46:6325.
[30] Maiti P, Yamada K, Okamoto M, Ueda K, Okamoto K. Chem Mater 2002;14:4654.
[31] Osman MA, Mittal V, Lusti HR. Macromol Rapid Commun 2004;25: 1145.
[32] Ray SS, Maiti P, Okamoto M, Yamada K, Ueda K. Macromolecules 2002;35:3104.
[33] Clearfield A, Berman JR. J Inorg Nucl Chem 1981;43:2141.
[34] Clearfield A, Duax WL, Medina AS, Smith GD, Thomas JR. J Phys Chem US 1969;73:3424.
[35] Clearfield A, Medina AS, Duax WL, Garces JM. J Inorg Nucl Chem 1972;34:329.
[36] Sun L, Boo WJ, Tien CW, Clearfield A, Sue HJ. Chem Mater, submitted for publication.
[37] Sun L, Boo WJ, Clearfield A, Sue HJ. New J Chem, submitted for publication.
[38] Sun L, Boo WJ, Browning RL, Sue H-J, Clearfield A. Chem Mater 2005; 17:5606.
[39] Sun L, Boo WJ, Sue HJ, Clearfield A. New J Chem 2007;31:39.
[40] Sue HJ, Gam KT, Bestaoui N, Spurr N, Clearfield A. Chem Mater 2004; 16:242.
[41] Boo WJ, Sun L, Liu J, Moghbelli E, Clearfield A, Sue HJ. J Polym Sci Part B Polym Phys, in press.
[42] Boo W-J, Sun L, Liu J, Clearfield A, Sue H-J. Compos Sci Technol 2007; 67:262.
[43] Sue HJ, Gam KT, Bestaoui N, Clearfield A, Miyamoto M, Miyatake N. Acta Mater 2004;52:2239.
[44] Kim HN, Keller SW, Mallouk TE, Schmitt J, Decher G. Chem Mater 1997;9:1414.
[45] Sue HJ, Pearson RA, Parker DS, Huang J, Yee AF. Abstr Pap Am Chem Soc 1988;196:62.
[46] Sue HJ, Yee AF. J Mater Sci 1993;28:2975.
[47] Agag T, Koga T, Takeichi T. Polymer 2001;42:3399.
[48] Ha B, Char K, Jeon HS. J Phys Chem B 2005;109:24434.
[49] Gam KT, Miyamoto M, Nishimura R, Sue HJ. Polym Eng Sci 2003;43: 1635.